Available online at www.sciencedirect.com
ScienceDirect
Physica A 387 (2008) 3563–3573
PHYSICA A
www.elsevier.com/locate/physa

Multifractal analysis of the UV/VIS spectra of malignant ascites: Confirmation of the diagnostic validity of a clinically evaluated spectral analysis

Irini S. Reljin[a], Branimir D. Reljin[a,*], Milka L. Avramov-Ivić[b], Dušan V. Jovanović[c], Goran I. Plavec[d], Slobodan D. Petrović[e,f], Gordana M. Bogdanović[g]

[a] *Faculty of Electrical Engineering, University of Belgrade, Bulevar Kralja Aleksandra 73, 11000 Belgrade, Serbia*
[b] *ICTM, Institute of Electrochemistry, University of Belgrade, Njegoševa 12/Karnegijeva 4, 11000 Belgrade, Serbia*
[c] *Institute of Oncology Sremska Kamenica, Department for Gastroenterology, Institutski put 4, 21204 Sremska Kamenica, Serbia*
[d] *Military-Medical Academy, Clinic for Lung Diseases and Tuberculosis, Crnotravska 17, 11000 Belgrade, Serbia*
[e] *Faculty of Technology and Metallurgy, Department of Organic Chemistry, Karnegijeva 4, 11000 Belgrade, Serbia*
[f] *Hemofarm Group, Pharmaceutical-Chemical Industry, 26300 Vršac, Serbia*
[g] *Institute of Oncology Sremska Kamenica, Experimental Oncology Department, 21204 Sremska Kamenica, Institutski put 4, Serbia*

Received 16 July 2007; received in revised form 26 December 2007
Available online 16 February 2008

Abstract

Multifractal (MF) approach was applied for the analysis of ultraviolet/visible (UV/VIS) spectra as an independent confirmation of the diagnostic efficacy of UV/VIS spectral analysis of intraperitoneal fluids, ascites, taken from patients with a known clinical diagnosis. Recently, it was reported that from UV/VIS spectra differentiation of malignant from benign ascites is possible. Here, it was shown that by using MF analysis of UV/VIS spectra, the objective classification of UV/VIS spectra is possible. The applicability of UV/VIS analysis and MF classification of spectra were evaluated on $N = 68$ cases, of which $M = 64$ and $B = 4$ were clinically confirmed as malignant and benign, respectively. The overall diagnostic efficacy was 89.71% when using on-line analysis of UV/VIS spectra (61 out of 68 samples were positively recognized: 58 malignant and 3 benign), and even 95.59% by using off-line MF classsification (65 out of 68 samples were classified correctly: 63 malignant and 2 benign). It can be inferred that UV/VIS spectral analysis of ascites, combined with MF analysis, could be suggested as a successful and safe screening method in the evaluation of intraperitoneal fluids.

Keywords: Ascites; Neoplasm; Medical diagnosis; UV/VIS spectroscopy; Fractals; Multifractal analysis

1. Introduction

Neoplastic and non-neoplastic diseases may cause the development of intraperitoneal fluid — ascites. Non-neoplastic causes of ascites are numerous: congestive heart failure, liver failure, renal or pancreatic disease,

* Corresponding author. Tel.: +381 11 3370 074; fax: +381 11 3248 681.
E-mail address: reljinb@etf.bg.ac.yu (B.D. Reljin).

0378-4371/$ - see front matter © 2008 Elsevier B.V. All rights reserved.
doi:10.1016/j.physa.2008.02.029

hypoproteinemia, chylous ascites from trauma or surgery, infectious processes and benign gynecologic conditions. The development of ascites in a patient with known cancer is most likely due to intraperitoneal spread of the disease. The term *malignant ascites* is used if neoplastic cells are identified in the fluid. Malignant ascites represent about 10% of all cases of ascites [1]. Approximately one-third of the patients with known malignancy have non-malignant causes of ascites, but in a patient with advanced cancer, the ascites is most likely malignant related [2].

Classic symptoms of ascites are abdominal distention and changes in abdominal girth. Signs of ascites, such as dullness to percussion, shifting dullness and fluid wave, may be totally absent in smaller effusions when ultrasonography, computerized tomography or endoscopic ultrasonography may be useful diagnostic tools. The use of laparoscopy in staging of abdominal cancers has increased the accuracy of determining malignant ascites and peritoneal disease. A peritoneal tap (drainage) is indicated when a definitive diagnosis of malignant ascites is required (for staging purposes or when surgical resection is planned based on the stage of the disease) and for determining the presence of malignant ascites in cancer patients with unknown intraperitoneal disease or in cryptogenic ascites [3].

Ascitic fluid is usually evaluated by cell count, various chemical analyses, and measurement of tumor and cytological markers. Cytological examination of peritoneal fluid yields a diagnosis in a large proportion of cases. The presence of elevated ascitic fluid to serum ratios of protein or lactic dehydrogenase, carcinoembryonic antigen, CA-125, fibronectin, cholesterol, human chorionic gonadotropin, or vascular endothelial growth factor favors malignancy [3–6].

When results of ascites cytologic analysis are negative, laparoscopy and biopsy have been used with great success in identifying the cause of ascites [3,7,8]. However, both methods are invasive and expensive.

Recently, it was very preliminarily shown [9] that it is possible to differentiate malignant, benign, and tubercular samples from a profile of ultraviolet/visible (UV/VIS) spectra of pleural effusion. Significant differences between malignant and benign spectra, defined by the number, shape and wavelength of the positions of the peaks, were observed when analyzing hundreds of different liquids. These preliminary results encouraged chemists to continue the investigation of the applicability of UV/VIS spectroscopy as a tool to gain additional confirmation of a final diagnosis. The UV/VIS method was further developed and with an additional invented procedure for the preparation of body liquids is patent protected [10,11] and a patent [11] was granted by the Russian federal patent office and by using obtained clinical results, this approach is suggested as a safe and reliable screening method [11,12].

In this study, the UV/VIS spectroscopy method was extended to the screening of ascitic fluids. Moreover, in addition to the exact evaluation of the UV/VIS spectra, based on the typical shape, number and precise positions of peaks (at always reproducible wavelength values) [10,11], the employment of multifractal (MF) analysis [13] for the classification of spectra is suggested here. From a number of reported papers [14–19], MF analysis is recommended as a powerful tool for the examination of both local and global features of the phenomenon under consideration.

UV/VIS spectroscopy and the employment of MF analysis for the evaluation of spectra and classification of samples were tested on samples taken from patients admitted to the Institute of Oncology Sremska Kamenica (Serbia) with ascites and having a known diagnosis. The obtained results are very promising, since the profiles of the UV/VIS spectra differed markedly (depending on the nature of the ascites) and highly corresponded to the clinical diagnosis, regardless the histological type of the malignant disease, indicating the applicability of these methods as additional tools in the diagnostic procedure.

The paper is organized as follows. A brief review of the methods (UV/VIS spectroscopy and MF analysis) employed for the classification of ascites is presented in Section 2. Section 3 is concerned with results obtained from analyses of the UV/VIS spectra of clinically collected ascites (68 cases). On-line classification and automatic off-line MF classification of the UV/VIS spectra are compared to the already derived clinical diagnoses. High reliability was obtained employing both classification methods.

2. Methods

2.1. UV/VIS spectroscopy

Ultraviolet/visible (UV/VIS) spectroscopy studies the absorption of electromagnetic radiation in the range of 200–800 nm (10^{-9} m). This spectroscopy is commonly named “electronic spectroscopy” because it comprises photon energies of 36–72 kcal/mole and in the near ultraviolet region it extends this energy range to 143 kcal/mole. These energies are sufficient to promote or excite a molecular electron to a higher energy orbital. Consequently, absorption

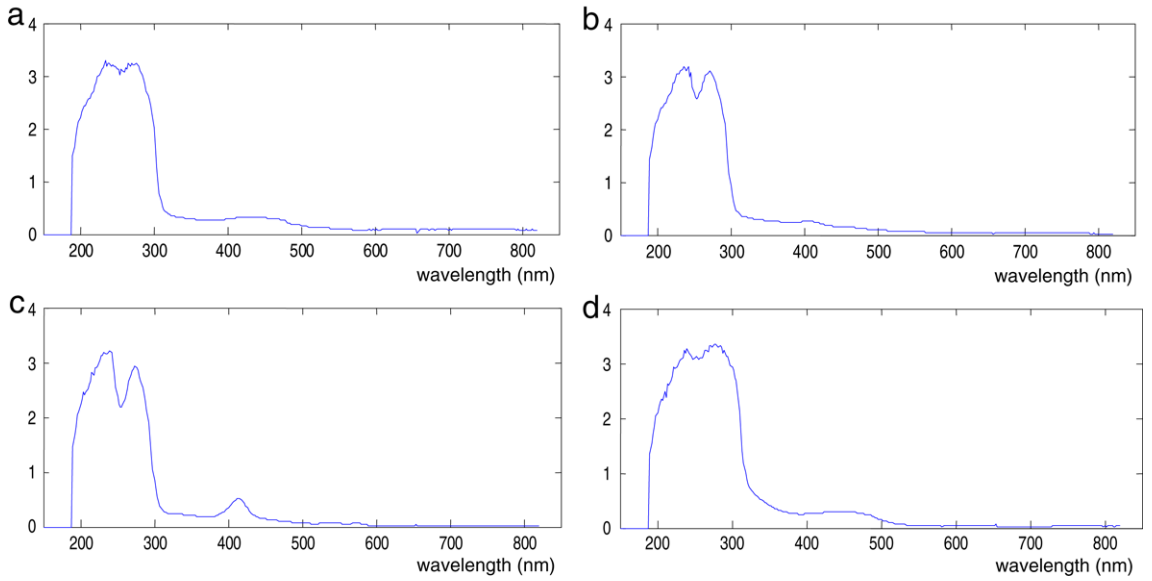

Fig. 1. Typical UV/VIS spectra of malignant ascites [11]: (a) ovarian cancer, (b) colon cancer, (c) cancer of unknown origin, (d) breast cancer.

spectroscopy carried out in this region is named "electronic spectroscopy". The advantages of UV/VIS spectroscopy over other spectroscopic methods are its high sensitivity (detection limit is 10^{-6} mol), simple instrument handling and relatively cheap instrumentation [20]. The content of an investigated sample strictly determines the profile of its UV/VIS spectrum, which is defined by the absorbance, A, according to the Lambert–Beer law [21]

$$A = \log_{10} \frac{I_0}{I} = \varepsilon_\lambda L c, \tag{1}$$

where I_0 is the incident light intensity, I is the amount of light transmitted through a solution, ε_λ is the molar absorbance (which depends on the wavelength λ), L is the length of the light path through the sample and c is the solution concentration. The profile of a UV/VIS spectrum A (λ) is characterized by a number of peaks at characteristic wavelengths, indirectly describing the content of the solution under investigation.

When applying UV/VIS analysis to intraperitoneal fluids, characteristic spectra are obtained, with significant differences between malignant and benign samples. Malignant ascites are characterized by two well-defined and well-shaped peaks in the wavelength range between 210 and 320 nm [9–12]. The peaks are wide, almost symmetrical, and sharp with a maximum absorbance value of A between 3 and 4. In the spectral region between 350 and 500 nm, a low plateau, with an absorbance value mostly below one is recorded [11]. As an illustration, four characteristic examples of UV/VIS spectra for malignant ascites are presented in Fig. 1: ovarian cancer (A), colon cancer (B), cancer of unknown origin (C) and the breast cancer (D).

In a case of non-malignant (benign) ascites, the UV/VIS spectrum is characterized by an array of sharp peaks recorded in the range from 210 to 320 nm. This region of undifferentiated peaks exhibits absorbance values mostly above 4 and never lower than 3.5. In the spectral region between 350 and 500 nm, a high plateau is seen with an absorbance value up to 2 [11]. A typical example of a UV/VIS spectrum for a benign sample is presented in Fig. 2.

As with other signals, UV/VIS spectra can be analyzed using a variety of signal processing methods. Usually, spectra are on-line compared by overlaying them to see how they differ or match. This an easy task if the spectra have multiple points of identification, e.g., peaks, troughs, shoulders. A match can be reported if the peak position and general shape are the same. If there is little spectral detail, instead of the original spectra, their first (or higher) derivative may help for better comparison. Derivative spectra are usually obtained by differentiating the recorded signal with respect to the wavelength as the spectrum is scanned [22].

Principal component analysis (PCA) is very often used for describing and differentiating multivariate signals. The PCA, originating from linear algebra and introduced by Pearson in signal analysis more than century ago [23], clusters an input data set into a few orthogonal variables according to their relevance on the total variance. The first PC (PC1)

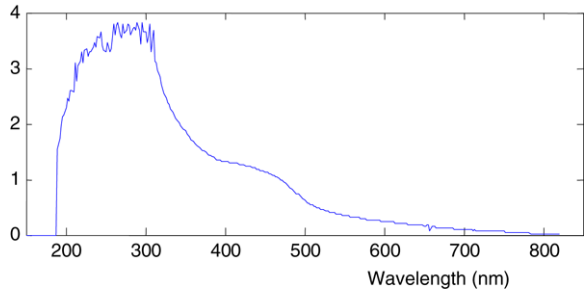

Fig. 2. Typical UV/VIS spectrum of benign ascite (Clinical diagnosis: Ovarian cysts).

represents the dominant part of the total variance of the input data, the second PC (PC2) accounts for the second largest amount of the variance while being orthogonal to PC1, and so on. Principal components are highly decorrelated, thus enabling the extraction and separation of different features from a recorded signal. Moreover, only the few first PCs support almost all of the variance (for example, more than 95%), making this method very useful in multivariate analysis. To determine which of the PCs represents variance due to a specific input pattern, the Wilcoxon ranked-sum test may be used as an appropriate statistics to test significant differences between input data [24,25]. Finally, from such preprocessed data, pattern classification is performed, usually with the assistance of artificial intelligence algorithm. A support vector machine (SVM), [26,27] is very often used for such a purpose [25], since this technique determines the optimal separating hyperplane that maximizes the margin between classes in a multidimensional data space.

2.2. *Multifractal analysis*

PCA/SVM-based algorithms are quite powerful in the classification of spectra, but they need complex calculations. In this research, the possibility of the employment of some other methods for the automatic evaluation and classification of ascites from their UV/VIS spectra was considered. Among several possible methods, we investigated the use of multifractal (MF) analysis, due to its possibility to describe numerically complex shapes and phenomena [13].

Fractal analysis is a robust method for describing events, structures or phenomena, having the fundamental feature known and referred to as *self-similarity*. In short, this feature means that, irrespective of the complexity of the shape of an object, by looking deeper and deeper into the structure, an observer can find the same (or similar) shapes on different scales. The classical example of such a structure is a coastline [28]. The fractal object may be characterized by its fractal dimension, D_f, a non-integer number, describing how the irregular structure of objects and/or phenomena is replicated in an iterative way from small to large scales [13,29]. A number of different methods for estimating the fractal dimension are known but the most popular one is the box-counting method [17,30]. This method involves covering a fractal with a grid of n-dimensional boxes with side length ε and counting the number of non-empty boxes, $N(\varepsilon)$. For covering fractal lines (one-dimensional signals), the grid is one of squares ($n = 2$), for covering fractal surfaces (two-dimensional signals, such as images), a grid of cubes ($n = 3$) is used and for covering fractal volumes (objects), a grid of hypercubes is used ($n = 4$). Boxes of recursively different sizes are used to cover the fractal. The limiting value of $N(\varepsilon)$, when ε tends to zero, follows the power law, $N(\varepsilon) \sim \varepsilon^{-D_f}$, i.e., the fractal dimension is estimated as

$$D_f = -\lim_{\varepsilon \to 0} \frac{\ln(N(\varepsilon))}{\ln(\varepsilon)}. \tag{2}$$

Fractal analysis is very efficient in describing objects or phenomena expressed in terms of two states; e.g., black–white, true–false, 0–1, etc. The fractal dimension is a good tool for characterizing the irregularity of a curve or a surface. However, if the phenomenon is more complex (such as, gray-scale images, meteorological signals, etc.) its characterization requires more general descriptors [15]. Consequently, the idea of self-similarity is extended from sets to measures. Instead of one measure, μ, describing a phenomenon regardless of the scale (when one considers fractals), a set of measures, $\Sigma\mu_i$, describing *statistically the same* phenomenon on different scales, is employed. In this case, one is considering multifractals [30]. From a multifractal spectrum, both local and global information of data regularity can be derived [14,15].

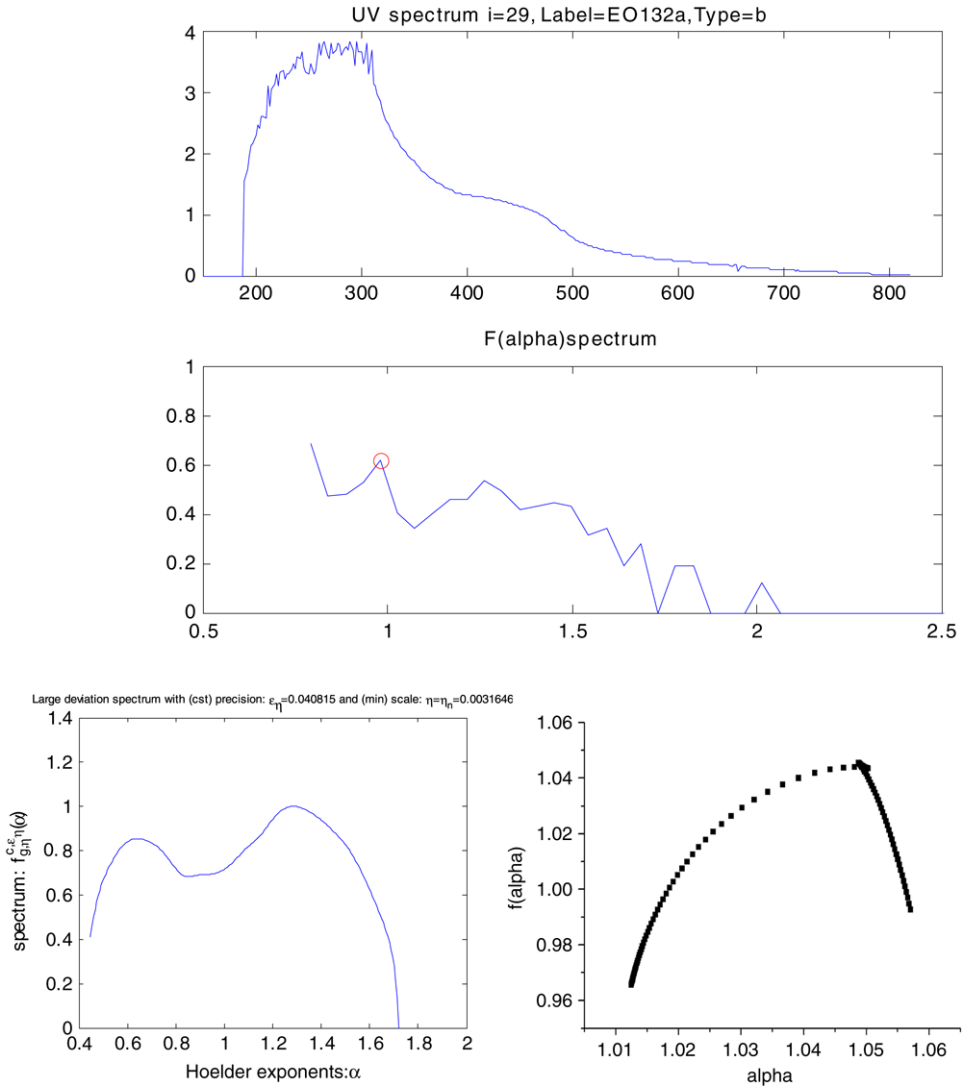

Fig. 3. UV/VIS spectrum of a benign ascite and the corresponding MF spectra obtained using HISTMF, FracLab (left) and Falpha (right).

The quantitative description of a multifractal property can be derived in several ways [30–36]. Usually, the procedure starts with finding the non-integer exponent α, known as the *Hölder exponent*, describing the point-wise singularity of the object, and then deriving the distribution of this quantity, known as the *multifractal spectrum*, $f(\alpha)$, as is briefly described below.

Let the structure (dataset) S be divided into non-overlapping boxes (subsets) S_i of size ε such that $S = \cup_i S_i$. Each box S_i is characterized by some amount of measure, $\mu(S_i)$. It should be shortly mentioned that a measure is the function that assigns different values to the subsets of a given set, where the value can represent for example a "size", a "probability" or an "intensity value", and the boxes may be assumed as measure domains. An equivalent parameter suggested for MF analysis is defined by

$$\alpha_i = \frac{\ln(\mu(S_i))}{\ln(\varepsilon)}, \tag{3}$$

which is denoted as the *coarse Hölder exponent* of the subset S_i. If ε tends to zero, the coarse Hölder exponent approaches the limiting value α at the observed point

$$\alpha = \lim_{\varepsilon \to 0}(\alpha_i). \tag{4}$$

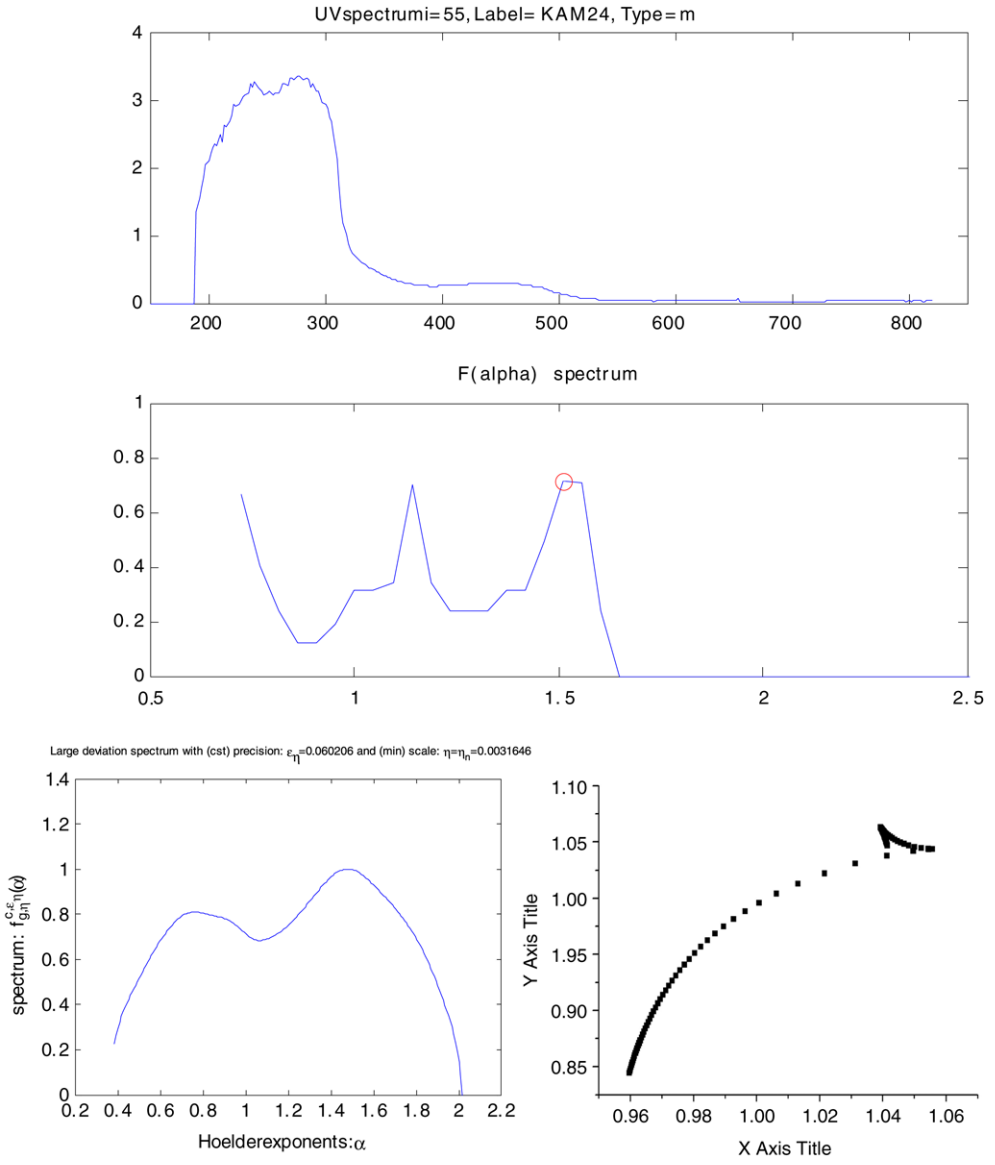

Fig. 4. UV/VIS spectrum of a malignant ascite and the corresponding MF spectra obtained using HISTMF, FracLab (left) and Falpha (right).

The parameter α depends on the actual position on the fractal and describes the *local regularity* of the structure. In the whole structure, there are usually many boxes (or points, in the limiting process) with the same parameter α. Consequently, it is possible to find the distribution of this quantity, i.e., to find the function $f(\alpha)$, known as the MF spectrum, over the subsets characterized by α. This function describes the *global regularity* of the observed structure. The MF spectrum can be assumed as the *fractal dimension* over the subsets characterized by α

$$f_\varepsilon(\alpha_i) = -\frac{\ln(N_\varepsilon(\alpha_i))}{\ln(\varepsilon)}, \tag{5}$$

where $N_\varepsilon(\alpha_i)$ is the number of boxes S_i containing a particular value of α_i. From Eq. (5), the limiting value of MF spectrum

$$f(\alpha) = \lim_{\varepsilon \to 0}(f_\varepsilon(\alpha)), \tag{6}$$

can be obtained. The MF spectrum $f(\alpha)$ calculated as above is known as the *Hausdorff dimension* of the distribution of α.

A number of methods to estimate the multifractal spectrum [30–36], based on geometrical or statistical properties of the data, both in the original and transformed space (for instance in Fourier and wavelet transform domains) have been reported. Some of the methods for the estimation of MF spectra are publicly available, for example, the program FracLab [34] derived from Levy Vehel, which is based on the large deviation theory, and the program Falpha from the Matpack packet derived by Gammel [35], which is based on the method of moments and Legendre transform, suggested by Chhabra and Jensen [36].

The programs FracLab and Falpha are quite powerful and describe well the global structure. However, they are not so efficient in describing some particular details from the input data, due to the averaged (smooth) MF spectrum $f(\alpha)$, as noticed in Ref. [19]. For extracting particular details from input data, a simple and direct way of computing the MF spectrum, known as the "histogram method" may be more useful. This method is briefly explained below.

For a given set (data), coarse Hölder exponents are calculated according to Eq. (3). Then a histogram of α is determined in the following manner. The whole α range from $\alpha_{\max}$ to $\alpha_{\min}$ is subdivided into R subranges of size $\Delta\alpha$

$$\Delta\alpha = (\alpha_{\max} - \alpha_{\min})/R. \tag{7a}$$

If the actual value of α lies within the subrange $r = 1, 2, \ldots, R$, i.e., if $\alpha_r \le \alpha < (\alpha_r + \Delta\alpha)$, it is replaced by α_r

$$\alpha_r = \alpha_{\min} + (r-1)\Delta\alpha, \quad r = 1, 2, \ldots, R. \tag{7b}$$

Then a histogram of α is calculated by covering the α-space by regular boxes with integer box size j. The boxes containing at least one value of α_r are counted giving the number $N_j(\alpha_r)$. Boxes of different sizes, $j = 1, 2, \ldots$, are recursively taken into consideration and the corresponding Hausdorff measures are calculated for each input data pattern according to Eq. (5), which now reads

$$f_j(\alpha_r) = -\frac{\ln N_j(\alpha_r)}{\ln(j)}, \quad j = 1, 2, \ldots. \tag{8}$$

In discrete space (as recorded signals usually are), the limiting values given by Eqs. (4) and (6) are not possible to calculate in a closed form, due to the discrete behavior of the box sizes: $\varepsilon = \varepsilon_i = i$, $i = 1, 2, \ldots$ (for determining α), and $j = 1, 2, \ldots$ (for determining $f(a)$). Also, the minimal box size equals 1. However, the values of α and $f(\alpha)$ can be estimated from bi-logarithmic plots of $\ln(\mu(S_i))$ versus $\ln(i)$, for α, and from $\ln(N_j(\alpha_r))$ versus $\ln(j)$, $j = 1, 2, \ldots$, for $f(\alpha)$. The slope of the linear regression curve in given plot estimates the value of α and $f(\alpha)$, respectively [19]. Note that for determining $f(\alpha)$, the index j is used instead of i, due to different structure of boxes when estimating α and $f(\alpha)$.

The number of α subranges, denoted as R, influences the accuracy of the multifractal spectrum. A small number of subranges have the effect of low-frequency filtering, yielding a smooth spectrum, but with low resolution and small "sharpness". Conversely, too many subranges produce a saw-toothed ("erratic") spectrum, but with more details. In the present research, a compromise solution with $R = 50$–100 was adopted.

The program HISTMF, based on the described method, was already derived for two-dimensional signals and applied to an image analysis [18,19]. Here, this program was adapted to one-dimensional signal analysis.

3. UV/VIS analysis of abdominal ascites

3.1. Materials and methods

In this study, 92 ascites were taken from 82 consecutive patients admitted in the Institute of Oncology, Sremska Kamenica (Serbia), in the period January 1998–October 2003. The ascites were collected during routine abdominal drainage, mostly performed for therapeutic reasons. The majority of the patients were with known malignant disease. Patients with various malignancy and different disease stages were included in the study. The predominant histological type of cancer was adenocarcinoma. Fourteen out of the 92 ascites were chylous or bloody and therefore unavailable for UV/VIS analysis. Among the remaining 78 ascites, ten were obtained from eight patients in repeated abdominal drainage. For statistical analyses, only first time-extracted ascites ($N = 68$) were included. From these samples $M = 64$ were from patients with confirmed malignant disease and $B = 4$ were benign. The patients were mainly female (49 out of 68, or 72.06%) with an average age of 63 (in the range 25–89). Male patients (19, or 27.94%) were of average age 56 (19–79). For all patients, average age was 60 (19–89). A substrate stabilization procedure of the

Table 1
Comparison between clinical diagnoses and results of UV/VIS analysis

Type of disease	Clinical diagnosis	UV/VIS results positive/negative
Malignant disease	64	58/6
Breast cancer	13	12/1
Ovarian cancer	17	16/1
Cancer of uteri	2	2/0
Stomach cancer	10	9/1
Colorectal cancer	4	4/0
Hepatocellular cancer	5	3/2
Pancreatic cancer	3	3/0
Bladder cancer	1	1/0
Melanoma	1	1/0
Non-Hodgkin lymphoma	2	2/0
Hodgkin lymphoma	1	1/0
Cancer of unknown origin	5	4/1
Benign diseases	4	3/1
Ovarian cysts	1	1/0
Cardiovascular diseases	2	2/0
Hernia abdominalis	1	0/1
Total	68	61/7

Table 2
Clinical statistical analysis of UV/VIS diagnoses

	No. of positive test results[a]	No. of negative test results[b]	Total
Malignant	58	6	64
Benign	1	3	4
Total	59	9	68

[a] True positive and false positive results.
[b] False negative and true negative results.

ascites was performed and their UV /VIS spectra recorded as previously described [10–12]. Detailed clinical data and comparison between the clinical diagnoses and evaluation of the UV/VIS spectra are presented in Table 1.

3.2. Results of UV/VIS classification

A comparison between clinical diagnoses and the results of UV/VIS analysis for 68 ascites is presented in Table 1. Clinical statistical analyses are given in Table 2. By on-line inspection of the UV/VIS spectra, in 58 out of 64 malignant samples, a malignant profile was recognized and positively classified (90.63%). Only 4 benign ascites were available for analysis and 3 of them (75%) were positively classified. Only one false positive result was recognized. In this way the overall true positive diagnoses were confirmed with an accuracy of 89.71% (61 out of 69 samples).

3.3. MF analysis of UV/VIS spectra

In this study, the multifractal approach was applied to the classification of UV/VIS spectra. MF spectra of the UV/VIS spectra, were derived by applying the program HISTMF [18], based on the histogram method described in Section 2.2, as well as by applying publicly available programs FracLab [34], and Falpha [35]. Two characteristic examples of UV/VIS signals, for benign and malignant ascites, and their MF spectra are depicted in Figs. 3 and 4, respectively.

As can be seen from Figs. 3 and 4, the MF spectra for benign and malignant sample are quite different if they are estimated by the HISTMF program: for the benign sample, the MF spectrum globally decreases with α, having a maximum near $\alpha = 1.0$ (denoted as a small circle over the MF plot), while for the malignant sample, the MF spectrum is bimodal with a maximum near to $\alpha = 1.5$. After application of the FracLab, MF spectra are without

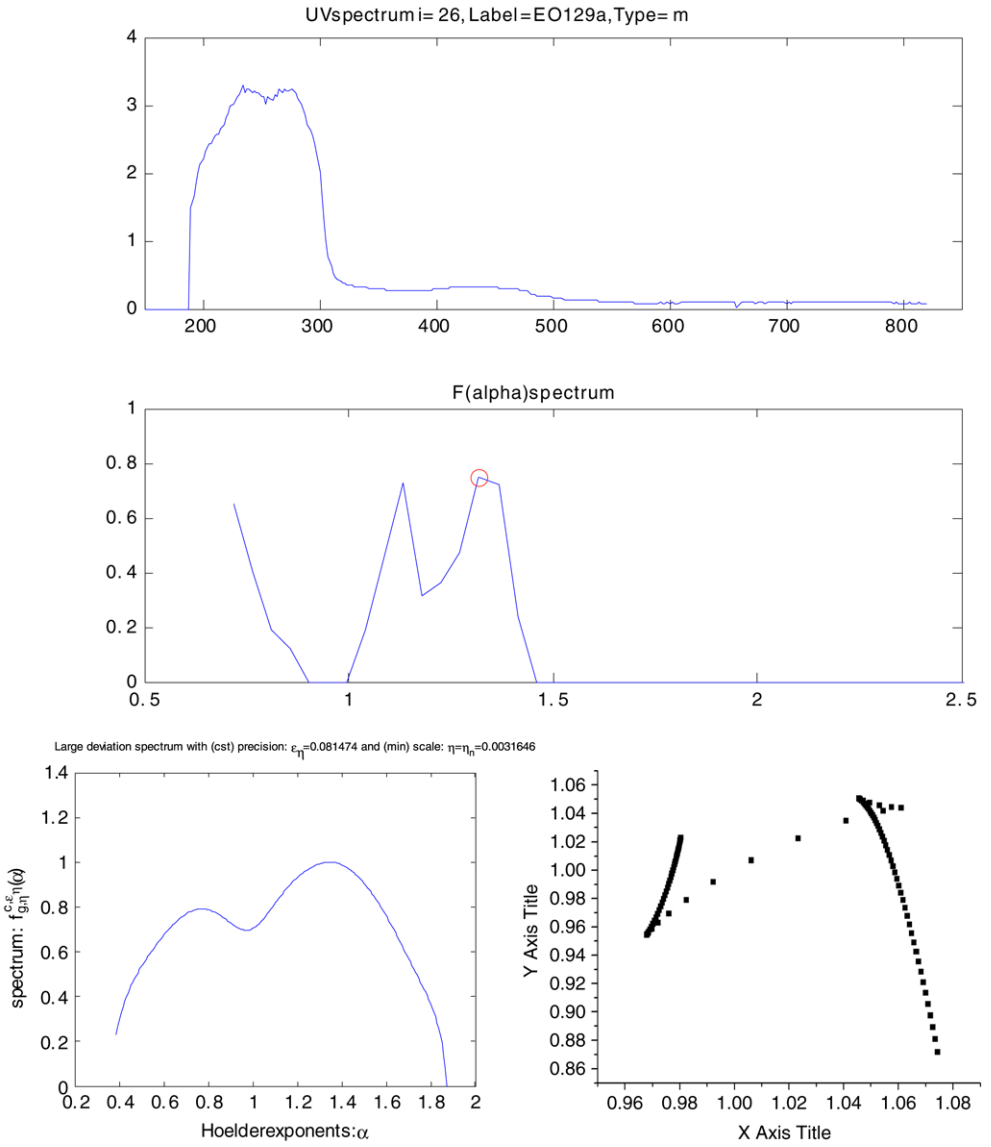

Fig. 5. UV/VIS spectrum of another malignant sample and the corresponding MF spectra obtained using HISTMF, FracLab (left) and Falpha (right).

visible difference, while they differ when Falpha was applied: for the malignant sample, the MF spectrum is left-sided. However, in general, this conclusion is not valid for other UV/VIS samples and MF spectra obtained with Falpha, while the MF spectra after HISTMF retain a global difference between the malignant and benign samples, as shown in Fig. 5 for a malignant sample. Due to these reasons, our further research was concentrated on the analysis of the MF spectra obtained by HISTMF and on the possibility that these spectra can help in the automatic classification of UV/VIS spectra.

Significant difference of MF spectra for malignant and benign ascites, numerically described by the value of the Hölder exponent α when $f(\alpha)$ has the maximum, was used as a relevant feature for the classification of UV/VIS spectra. The whole collection of UV/VIS spectra (68 samples) was processed by using a program HISTMF. Then the obtained set of MF spectra was divided randomly into two parts: a training set and a test set having one-half of the MF samples each (32 malignant and 2 benign samples). From the training set, the threshold value of α, $\alpha_T = 1.2$, which separates malignant samples from benign was found: samples having a maximum in the MF spectrum at value of

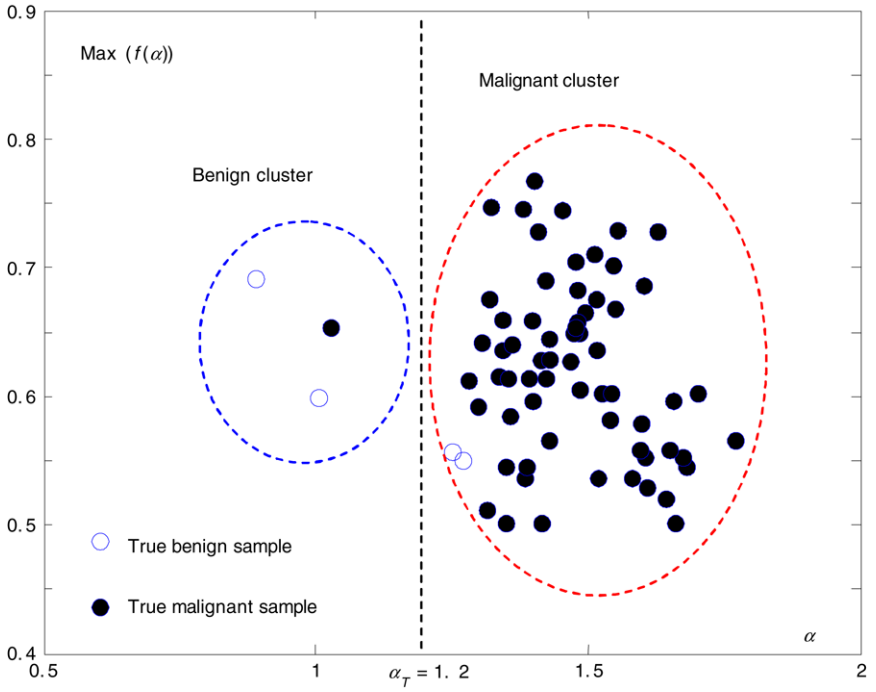

Fig. 6. Plot of the maximum of the MF spectra versus the Hölder exponent α for the given set of $N = 68$ clinically collected ascites. Malignant samples are denoted as black dots.

the Hölder exponent greater than the threshold limit α_T, are classified as malignant, otherwise, the sample is benign. Subsequently, the test set was used for evaluation. From the test set, two benign samples were falsely classified as malignant, while only one of malignant samples was falsely classified. The scattered plot of the maximum of the MF spectra (drawn as circles, for true benign samples, and as black dots, for malignant samples) versus the corresponding values of the Hölder exponent α is depicted in Fig. 6. True malignant samples are clearly clustered around the value of $\alpha = 1.5 \pm 0.25$.

As can be seen from Fig. 6, with the threshold of $\alpha_T = 1.2$, the separation of maximums of MF spectra and thus the classification of the UV/VIS spectra for the given set of ascites, is possible. In our study 63 out of 64 malignant samples were classified as true positive (98.44%), with one false negative result. Classification of the benign samples was less accurate: 2 out of 4 benign samples (50%) were falsely positively classified. The overall true positive diagnoses were confirmed by MF method in 65 out of 68 cases (95.59%). Note that in this study, only a small number of benign ascites were available, which was insufficient to derive a statistically significant conclusion. However, in the previously derived study [12] over 50 benign pleural effusions were analyzed regarding diagnostics in pulmonology, and their UV/VIS spectra highly corresponded to the clinical diagnoses, having (almost) the same profile as depicted in Fig. 2.

4. Conclusions

In this paper the applicability of UV/VIS spectral analysis of malignant ascites was investigated. The aim was to check whether this method could be used as a supplementary screening procedure for determining the presence of malignant ascites in patients with unknown intraperitoneal disease. The obtained results showed that UV/VIS spectra highly correspond with the clinical diagnosis regardless the histological type of the malignant disease. Moreover, MF analysis of the UV/VIS spectra leads to even more accurate off-line classification of UV/VIS spectra. In conclusion, it can be inferred that UV/VIS spectral analysis of ascites, combined with MF analysis, could be recommended as a successful and safe screening method in the evaluation of intraperitoneal fluids. In addition, the required instrumentation is relatively simple and non-expensive and the method is simple and fast. Also, the suggested method could be of special importance in uncertain and urgent cases presenting intraperitoneal fluid.

References

[1] B.A. Runyon, Care of patients with ascites, N. Engl. J. Med. 330 (1994) 337–342.
[2] B.A. Runyon, Malignancy-related ascites and ascitic fluid humoral tests of malignancy [Editorial], J. Clin. Gastroenterol. 18 (1994) 94–98.
[3] R.B. Hostetter, F.M. Marincola, D.J. Schwartzentruber, Treatment of metastatic cancer: Section 6. Malignant ascites, in: Vincent T. DeVita Jr, Samuel A. Rosenberg (Eds.), Cancer: Principles and Practice of Oncology, 7th edition, Lippincott Williams & Wilkins, Philadelphia, 2005 (Electronic version, CD).
[4] S. Bansai, K. Kaur, A.K. Bansai, Diagnosing ascitic etiology on a biochemical basis, Hepatogastroenterology 45 (1998) 1673–1677.
[5] B.K. Zebrowski, W. Liu, K. Ramirez, et al., Markedly elevated levels of vascular endothelial growth factor in malignant ascites, Ann. Surg. Oncol. 6 (1999) 373–378.
[6] S.L. Parsons, S.A. Watson, R.J.C. Steele, Malignant ascites, Br. J. Surg. 83 (1996) 6–14.
[7] C.M. Chu, S.M. Lin, S.M. Peng, C.S. Wu, Y.F. Liaw, The role of laparoscopy in the evaluation of ascites of unknown origin, Gastrointest Endosc. 40 (1994) 285–289.
[8] Q.S. Ringenberg, D.C. Doll, T.S. Loy, J.W. Yarbro, Malignant ascites of unknown origin, Cancer 64 (1989) 753–755.
[9] M. Avramov-Ivić, J. Zdravković, D. Vuković, U. Mioč, G. Bogdanović, UV-VIS spectroscopic investigations of pleural effusions: A possible screening diagnostic method for the differentiation of malignant from non-malignant effusions, Arch. Oncology 7 (1999) 27–28.
[10] S.D. Petrović, M. Avramov-Ivić, Individual substrate stabilization procedure for spectroscopic detection of tuberculosis and a new diagnostic method, (2003-12-03), PCT/YU 03/00006, 2003.
[11] S. Petrović, M. Avramov-Ivić, Metod stabilizaciji individualnogo substrata dlja spektraljnogo opredeljenija zlokacestvenosti, Russian Federation, Federal Institution for Intellectual Rights, Patent Ru No 2285443C2, pp. 1–11, 20. 10. 2006.
[12] G. Plavec, M. Avramov-Ivić, S.D. Petrović, I. Tomić, O. Lončarević, D. Jovanović, UV/VIS spectrophotometry as a screening method for malignancy in pleural effusion, in: ERS Annual Congress, 17–21 Sep 2005, European Respiratory J. 26 (Suppl. 49/735) (2005) 562.
[13] H-O. Peitgen, H. Juergens, D. Saupe, Chaos and Fractals, second edition, Springer, 2004.
[14] J. Lévy Véhel, P. Mignot, Multifractal segmentation of images, Fractals 2 (3) (1994) 379–382.
[15] J. Lévy Vehel, Introduction to the multifractal analysis of images. http://www-ocq.inria.fr/fractales,1996.
[16] P. Iannaccone, M. Khokha (Eds.), Fractal Geometry in Biological Systems, CRC Press, 1996.
[17] M. Turner, J. Blackledge, P. Andrews, Fractal Geometry in Digital Imaging, Academic Press, 1998.
[18] I. Reljin, B. Reljin, I. Pavlović, I. Rakočević, Multifractal analysis of gray-scale images, in: Proc. IEEE Conf. MELECON-2000, vol. II, Cyprus, 2000, pp. 490–493.
[19] T Stojić, I. Reljin, B. Reljin, Adaptation of multifractal analysis to segmentation of microcalcifications in digital mammograms, Physica A: Statistical Mech. Appl. 367 (2006) 494–508.
[20] M.J.K. Thomas, Ultraviolet and Visible Spectroscopy, second ed., Willey, 1996.
[21] K-E. Peiponen, T. Asakura, UV-Visible Reflection Spectroscopy of Liquids, Springer, 2004.
[22] P. Minkiewicz, B. Pliszka, J. Dziuba, J. Oszmianski, Second and third derivatives of UV spectra as a tool for identification of major anthocyanins from Aronia Melanocarpa extract, separated using reversed-phase high-performance liquid chromatography, Collection of Czechoslovak Chem. Commun. 69 (7) (2004) 1443–1452.
[23] K. Pearson, On lines and planes of closest fit to systems of points in space, Phil. Mag. 2 (1902) 559–572.
[24] N. Ramanujam, M.F. Mitchell, A. Mahadevan-Jansen, et al., Cervical precancer detection using a multivariate statistical algorithm based on laser-induced fluorescence spectra at multiple excitation wavelengths, Photochem. Photobiol. 64 (1996) 720–735.
[25] T.M. Breslin, Fushen Xu, Gregory M. Palmer, C. Zhu, K.W. Gilchrist, N. Ramanujam, Autofluorescence and diffuse reflectance properties of malignant and benign breast tissues, Ann. Surgical Oncology 11 (1) (2003) 65–70.
[26] V. Vapnik, Statistical Learning Theory, Wiley-Interscience, New York, 1998.
[27] C. Burges, A tutorial on support vector machines for pattern recognition, Data Mining Knowledge Discovery 2 (1998) 121–167.
[28] B.B. Mandelbrot, How long is the coast of Britain? Statistical self-similarity and fractional dimension, Science 156 (1967) 636–638.
[29] B.B. Mandelbrot, The Fractal Geometry of Nature, W. H. Freeman, Oxford, 1983.
[30] D. Harte, Multifractals: Theory and Applications, Chapman and Hall, 2001.
[31] P. Goncalves, R. Riedi, R. Baraniuk, A simple statistical analysis of wavelet-based multifractal spectrum estimation, in: Proc. 32nd Conf. on Signals, Systems and Computers (Asilomar), Monterey, 1998.
[32] R. Riedi, R.H. Riedi, M.S. Crouse, V.J. Ribeiro, R.G. Baraniuk, A multifractal wavelet model with application to network traffic, IEEE Trans. Inform. Theory 45 (4) (1999) 992–1018.
[33] P. Kestener, J. Marc Lina, P. Saint-Jean, A. Arneodo, Wavelet-based multifractal formalism to assist in diagnosis in digitized mammograms, Image Anal. Stereol. 20 (2001) 167–174.
[34] FracLab: A fractal analysis toolbox for signal and image processing. http://www2.irccyn.ec-nantes.fr/FracLab/index.html.
[35] B.M. Gammel, Falpha — The $f(\alpha)$-Spectrum Analyzer. http://users.physik.tu-muenchen.de/gammel/matpack/tools/Falpha/.
[36] A. Chhabra, R.V. Jensen, Direct determination of the $f(\alpha)$ singularity spectrum, Phys. Rev. Lett 62 (1989) 1327–1330.